

1 Rotten to the core? How internal stem damage varies vertically in savanna trees and 2 is influenced by tree species, traits, and external damage pressures

3
4 Abbey R. Yatsko^{1*}, Habacuc Flores-Moreno³, Michaela Fitzgerald⁴, Amy E. Zanne^{1,2}

5
6 ¹ Biology Department, University of Miami, Coral Gables, Florida, USA

7 ² Cary Institute of Ecosystem Studies, Millbrook, New York, USA

8 ³ CSIRO Health and Biosecurity, Brisbane, Queensland, Australia

9 ⁴ SUNY College of Environmental Science and Forestry, Syracuse, New York, USA

10 11 **Abstract**

- 12 1. Trees are important aboveground carbon sinks in savanna ecosystems, yet consumption of
13 internal wood by decomposers (e.g., termites and microbes) creates uncertainties in tree biomass
14 accounting. It remains unclear whether internal stem damage is constant or variable throughout
15 the tree, making it uncertain if a lower stem sample reflects damage in the entire tree.
16 Furthermore, total damage and damage location are likely influenced by external damage
17 pressures (i.e., termites, microbes, and fire), tree species and tree traits (i.e., diameter at breast
18 height (DBH), wood density), and their interactions.
- 19 2. We sampled internal damage in the lower stem of savanna trees in North Queensland, Australia to
20 test for vertical variation in terms of proportional and absolute amount of damage. We compared
21 damage estimates from a single-sample method, assuming constant damage, with a multi-sample
22 method, assuming variable damage, to test how well one sample represents the lower stem. We
23 investigated if tree species accumulated damage differently based on their traits (i.e., DBH and
24 wood density) or susceptibility to external damage pressures (i.e., fire scarring and termite
25 presence). Finally, we tested if external damage pressures differentially affected tree species and
26 if this was mediated by tree traits.
- 27 3. The absolute amount, but not proportion, of damage decreased with higher vertical position on
28 the stem. There was no difference in total stem damage between the single-sample and multi-
29 sample methods. Species-specific variation in internal stem damage was influenced by DBH and
30 wood density. Total damage was greatest in large trees, particularly those with external termite
31 presence. Finally, external termite presence, but not fire scarring, differentially affected tree
32 species and was most likely to occur on large, dense trees.
- 33 4. *Synthesis.* We demonstrated that a single sample effectively captured total internal damage in the
34 lower stem. Although species differed in total damage, damage accumulation rates with height
35 were consistent, suggesting a general relationship. By integrating the influence of external factors
36 and tree traits, our findings underscore the importance of considering these elements for
37 accurately estimating carbon stored in aboveground tree biomass.

38 39 **Introduction**

40 Savannas cover 20% of the Earth's terrestrial surface and are ecologically rich ecosystems with unique
41 biogeochemistry (Scholes & Archer 1997), yet are often overlooked for their role in the global carbon
42 cycle (Parr et al., 2014; Dobson et al., 2022). In the savanna, woody plants store carbon both while alive
43 and dead; living trees sequester an estimated 0.39 Pg C every year (Grace et al., 2006), and dead wood

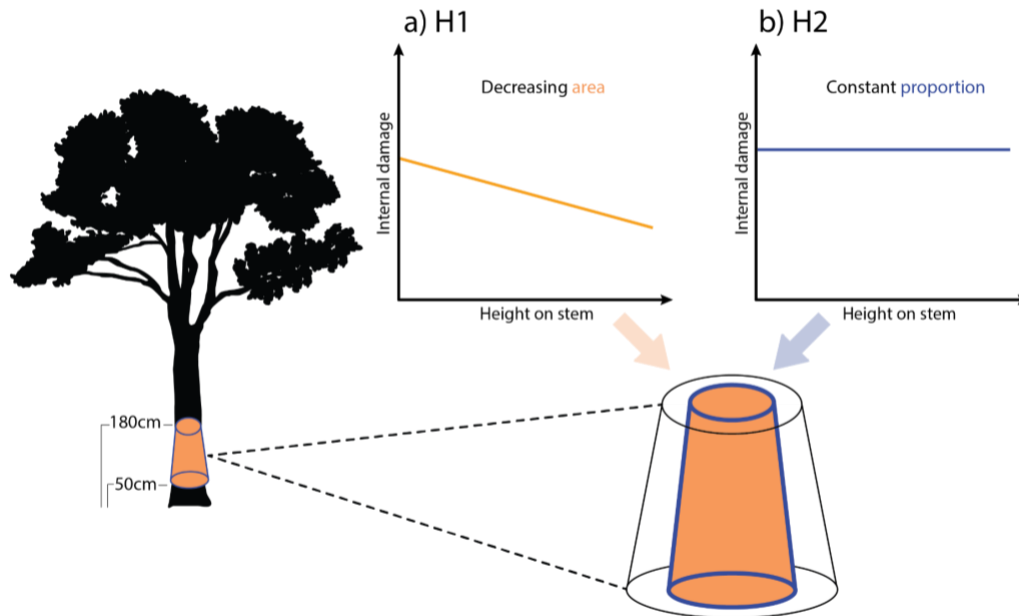
44 stores a further 9.6 Pg C globally (Wijas, Allison et al., 2024). In terms of savanna carbon storage, woody
45 plant aboveground biomass (AGB) is of particular interest due to its longevity on the landscape. Yet,
46 AGB is eventually cycled back to the atmosphere and soils via the decomposition process (Zhou et al.,
47 2007), of which termites and fire are especially important contributors in savanna ecosystems (Zanne et
48 al., 2022; Murphy et al., 2023).

49
50 While many studies focus on carbon storage in living trees (Sullivan et al., 2017) and carbon turnover via
51 decomposition of downed deadwood (Wijas, Flores-Moreno et al., 2024), internal tree stem damage is a
52 component of savanna ecosystem that is largely overlooked in carbon cycling models (Calvert et al.,
53 2024). Internal stem damage occurs when wood within living trees decomposes (Janzen 1976) and has
54 been documented to affect up to a third of savanna tree AGB (Flores-Moreno et al., 2024), resulting in
55 uncertainties in tree AGB estimation (Calvert et al., 2024). Termite decay (Eleuterio et al., 2020; N'Dri et
56 al., 2011; Werner & Prior 2007; Yatsko et al., 2024) and microbial 'heartrot' (Lee et al., 1988; Zeps et al.,
57 2017; Heineman et al., 2015; Eleuterio et al., 2020; Yatsko et al., 2024) contribute to internal stem
58 damage, yet its concealed nature makes measurement challenging. To quantify total damage and
59 determine where it occurs, destructively harvesting trees proves useful (Calvert et al., 2024), however this
60 is often logistically infeasible and cannot be carried out extensively. Nondestructive sampling is more
61 accessible, using increment corers (Heineman et al., 2015), resistograph drills (Flores-Moreno et al.,
62 2024), and sonic tomography (Gilbert et al., 2016) to target sampling in the lower stem or at diameter at
63 breast height (DBH) (Brown et al., 1995; Zeps et al., 2017; Eleuterio et al., 2020; Werner and Prior 2007;
64 Flores-Moreno et al., 2023). However, it may be problematic to assume that a single measurement
65 represents damage throughout the entire tree (Flores-Moreno et al., 2023), and capturing vertical variation
66 would require a revised sampling strategy. If the amount of internal damage varies between different parts
67 of the tree, possibly due to different decomposers, it is important to account for these changes when
68 modeling damage.

69
70 Towards the goal of understanding vertical variation in internal stem damage, it is important to consider
71 how biotic players (mainly microbes and termites, Yatsko et al., 2024) cause internal stem damage and
72 partition wood resources within trees. From only two studies on internal stem damage vertical variation
73 (Calvert et al., 2024; Yatsko et al., 2024), two non-exclusive hypotheses emerge regarding vertical
74 damage variation, which depend on how damage is quantified. The first internal damage pattern
75 hypothesis is that damage (quantified as an absolute amount of wood) is concentrated at the tree base (see
76 **H1**, Figure 1a). Here, wood resources are high, since stem diameter is largest, and accessible to ground-
77 colonizing organisms. For instance, termites are usually foraging on the ground and may use the bottom
78 of tree stems as an access point to internal wood or enter through the roots, concentrating damage in the
79 lower stem (Yatsko et al., 2024). Furthermore, the amount of wood consumed by microbes has been
80 positively related to the amount of wood available (Gilbert et al., 2016); decomposers are often targeting
81 tree heartwood (Perry et al., 1985), which is greatest toward the bottom of the tree and can completely
82 disappear in fine branches (Climent et al., 2003).

83
84 The second internal damage pattern hypothesis is that damage, as a proportion, remains constant through
85 the lower stem to maintain a strong structure. This hypothesis largely relates to termite-driven internal
86 damage, as some wood-feeding termites live in the same tree that they consume (Werner & Prior 2007),
87 leading to a need to maintain a structurally strong home (see **H2**, Figure 1b). We expect that termites will

88 excavate wood in a constant proportion across vertical positions in the lower stem, leaving behind a
 89 strong structure to continue to live in. This has been described by termite tree ‘piping’, where stems are
 90 hollowed out like a straw (Werner & Prior 2007), and likely protects termites nesting inside the stem.
 91 While extensive hollowing (proportion > 0.6) can increase tree mortality (Werner & Prior 2007), it has
 92 been shown that trees with moderate, proportionally constant internal damage can maintain stability
 93 (Mattheck et al., 1994), especially if outer wood density is high (Larjavaara & Muller-Landau 2010;
 94 Osazuwa-Peters et al., 2014).



95
 96 Figure 1: a) Visualization for **H1** (‘damage at the base’): Internal damage (yellow line) is greatest at the
 97 tree base where the diameter is largest. b) Visualization for **H2** (‘strong home’): Internal damage as a
 98 proportion (purple line) remains constant at all heights, but decreases in absolute amount due to stem
 99 taper. Both **H1** and **H2** represent predictions for the lower stem (sampled between 50 and 180 cm, shown
 100 on left).

101
 102 To accurately estimate total internal stem damage and its vertical variation in the tree, it is necessary to
 103 consider variation across tree species, and if variation in damage accumulation across species is driven by
 104 underlying tree traits. Flores-Moreno et al. (2024) found that species with high wood density accumulated
 105 greater internal stem damage across a tropical rainfall gradient. Dense wood is preferred by *Coptotermes*
 106 *acinaciformis* (Oberst et al., 2018), which is known to hollow trees in Australian savannas. Such a
 107 preference may lead to tree species with dense wood accumulating more damage. Tree size (here, DBH)
 108 is also of importance; some studies found that larger trees had more frequent damage (Nogueira et al.,
 109 2006; Heineman et al., 2015), yet others found weak relationships between DBH and total damaged
 110 biomass (Flores-Moreno et al., 2024). Ultimately, understanding how internal stem damage varies across
 111 different tree species, and identifying tree traits responsible for these differences, remains a key challenge
 112 in characterizing internal stem damage.

113
 114 Beyond tree properties, external damage pressures such as fire and termite activity may also impact
 115 damage accumulation by facilitating access to internal wood. Fire is important for woody biomass
 116 turnover in savannas (Grace et al., 2006; Wijas, Allison et al., 2024), and external openings from fire

117 scarring may allow decomposers access to internal wood (N'Dri et al., 2011). The presence or absence of
118 fire scarring could lead to differences in both vertical variation of internal stem damage as well as total
119 damage accumulation. A study in an African savanna concluded that fire was a main 'cavity-opening
120 agent' in tree stems, allowing subsequent termite or microbial entry. Basal fire scarring is even a
121 management strategy that accelerates hollow formation for the benefit of hollow-dwelling fauna (Adkins
122 2006). External termite presence may also indicate trees undergoing internal damage. Termites build mud
123 tubes, tunnels or 'runways' externally on trees, which indicate infestation (Li et al., 2016), and termite
124 colonies built at the tree base can indicate internal hollowing (Eleuterio et al., 2020). Therefore, the
125 presence of external fire scarring and termite activity on tree stems may be an important predictor of
126 internal stem damage.

127

128 In this study, we measured internal damage at multiple vertical positions in the lower 2 m of tree stems in
129 a North Queensland, Australia savanna dominated by Myrtaceae flora. In this system, fire, termites and
130 microbes all contribute to wood decay (Clement et al., 2021; Law et al., 2023; Wijas, Flores-Moreno et
131 al., 2024) and extensive internal stem damage has previously been reported (Flores-Moreno et al., 2023).
132 We address the following questions:

133

134 Q1) Does the amount of internal damage change with a) vertical position on the lower stem
135 across species or b) vertical position on the lower stem for trees of different wood density and
136 DBH? We express damage as an absolute amount to test **H1** ('damage at the base'), and damage
137 as a proportion to test **H2** ('strong home').

138

139 Q2) Do estimates of total lower stem damaged biomass change based on vertical variation being
140 accounted for (via a multi-sample method) or not (via a single-sample method)?

141

142 Q3) Do species differ in total lower stem damaged biomass, and, if so, is this driven by tree traits
143 and/or external damage pressures?

144

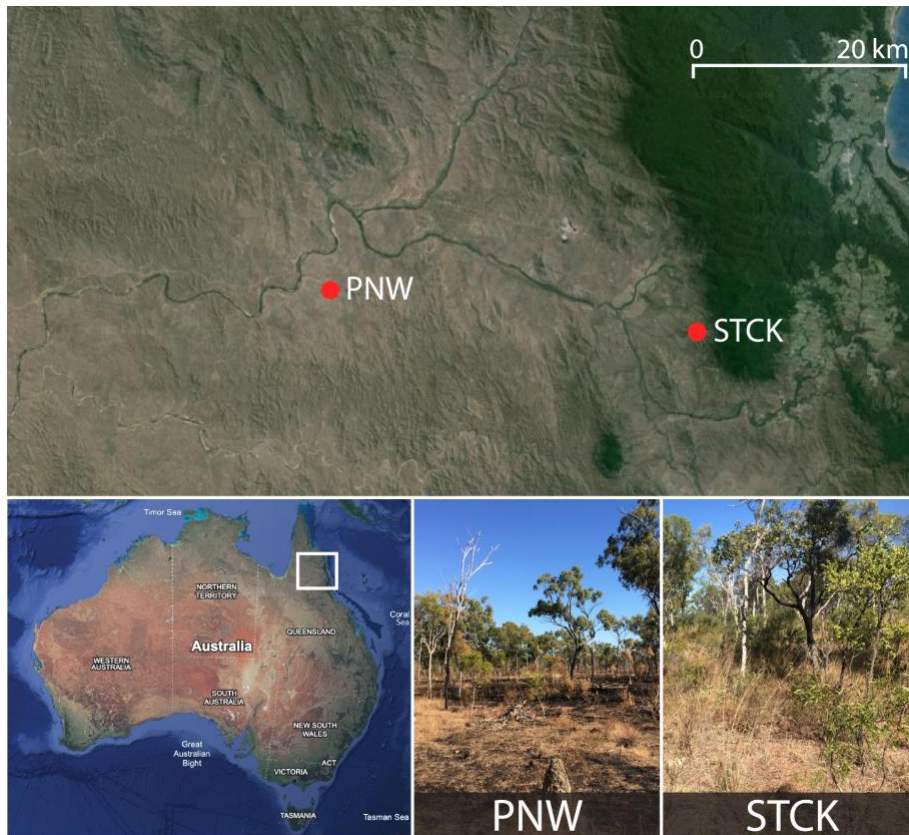
145 Q4) Do external damage pressures differentially affect tree species, and are detected differences
146 driven by underlying tree traits?

147

148 **Materials and Methods**

149 *Study site and sampling*

150 Sampling took place at two savanna sites in far north Queensland, Australia, Station Creek (STCK, -16.61
151 S, 145.24 E) and Pennyweight Station (PNW, -16.57 S, 144.92 E), located on the Australian Wildlife
152 Conservancy (AWC) Brooklyn Sanctuary (Figure 2). PNW is a drier savanna ecosystem (812 mm rainfall
153 annually) compared to STCK (1,728 mm of rainfall annually) (Cheesman et al., 2018). Both sites
154 experience a distinct wet and dry season, with 77% of rainfall occurring between November and April
155 (Cheesman et al., 2018).



156
 157 Figure 2. Location of Station Creek (STCK) Pennyweight Station (PNW) in far north Queensland,
 158 Australia and characteristic landscapes for each site.
 159

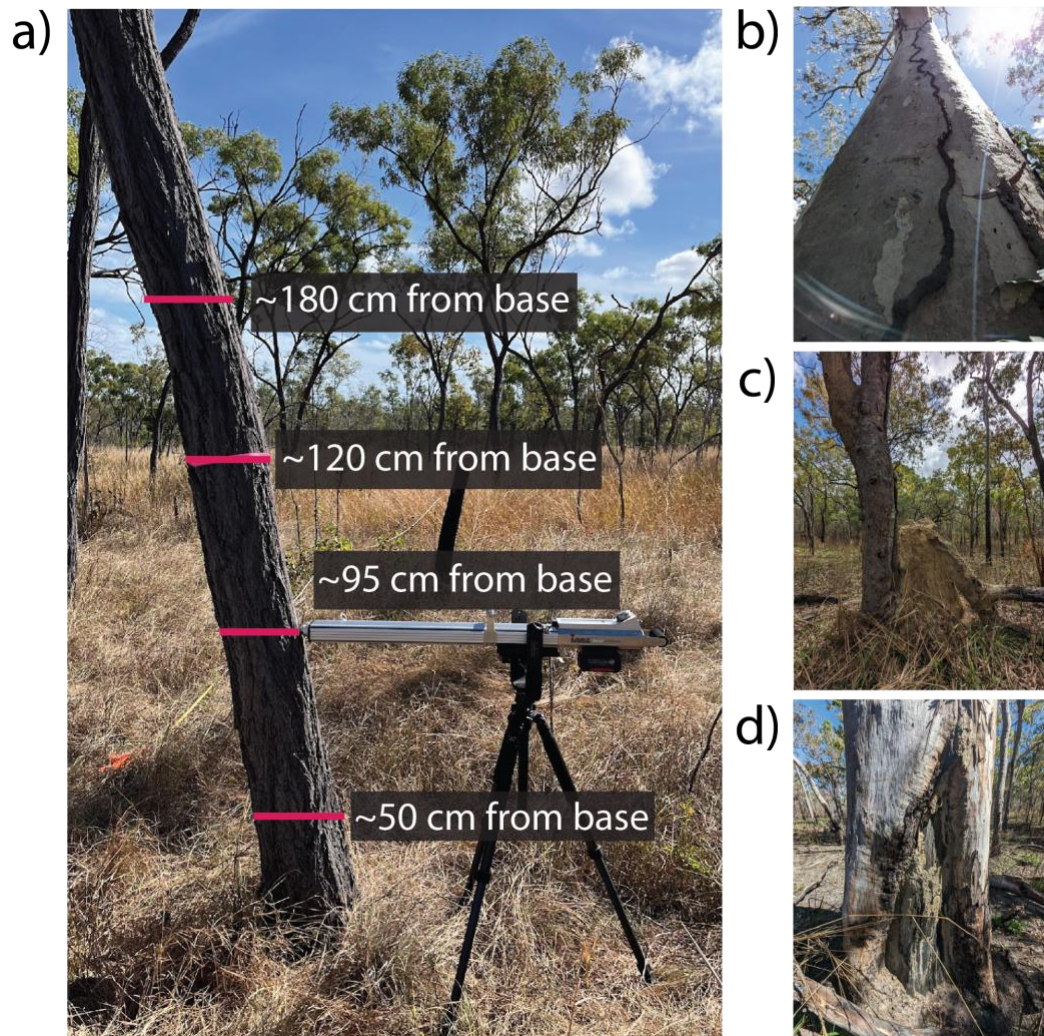
160 In 2018, 50x50 m plots were established at each site and DBH measurements and species identification
 161 were made for all trees in the plot. Wood density values for each species were extracted from the Tree
 162 Functional Attributes and Ecological Database (Supplementary Table 2, Harja et al., 2019). PNW is
 163 dominated by *Eucalyptus cullenii* and *Melaleuca stenostachya* (Myrtaceae), while STCK is more diverse,
 164 but largely dominated by *E. cullenii* and *Corymbia clarksoniana* (Myrtaceae) (Supplementary Table 1).
 165

166 We selected tree species with high biomass representation to investigate vertical stem damage variation,
 167 including three Myrtaceae species. We targeted species with known high levels of high internal stem
 168 damage (exceeding 30% of tree biomass damage described by Flores-Moreno et al., 2024) in order to
 169 determine vertical patterns of internal damage.
 170

171 We selected tree species with high plot-level biomass representation and known occurrence of internal
 172 stem damage (up to 30%, Flores-Moreno et al., 2024) to examine vertical patterns of stem damage. We
 173 selected three Myrtaceae species: *E. cullenii* (occurring at both sites: STCK, 65% of plot-level biomass,
 174 PNW, 96% of plot-level biomass), *M. stenostachya* (PNW, 2.3% of plot-level biomass), *C. clarksoniana*
 175 (STCK, 20% of plot-level biomass, Supplementary Table 1). We measured vertical variation of internal
 176 damage on the lower 2 m of stem for 45 trees (*E. cullenii* n = 21, *C. clarksoniana* n = 14, *M. stenostachya*
 177 n = 10), sampling at least 10 individuals per species in four vertical positions (Supplementary Table 2).
 178

179 *Quantifying internal stem damage*

180 We used an IML-RESI power drill to quantify internal damage (residrill; PD-500, IML, Germany, Figure
181 3a). The residrill measures resistance as the stylus turns, generating a resistograph measurement where
182 high resistance indicates sound wood and low resistance indicates damaged or decaying wood (see
183 Supplementary Figure 1). We drilled along the north-to-south plane at four vertical positions on each tree
184 (targeting sampling at approximately 50 cm, 95 cm, 120 cm, and 180 cm from the tree base, Figure 3a).
185 We recorded the DBH of the tree, the stem diameter at drilling point, as well as the distance from the
186 drilling point to the ground.



187
188 Figure 3. a) Internal stem damage sampling at four positions on the lower stem (approximately 50, 95,
189 120, and 180 cm above tree base); residrill pictured in the lower right. External termite presence via b)
190 runways on tree bark and c) a mound built at the base of the tree. d) External fire damage via basal
191 scarring.

192
193 For each measurement point, we quantified damage as an absolute amount (via area of the sampled cross
194 section, to address *H1*) and as a proportion (to address *H2*). To begin, we calculated damage as a
195 proportion from the residrill output data. A sound wood threshold was classified for each residrill sample
196 ('trace', Supplementary Figure 1). Internal stem damage was quantified as the percentage change from the

197 sound wood threshold (Flores-Moreno et al., 2024). Each trace was segmented using a piecewise function
198 to minimize residual sum of squares (RSS). For each trace, we compared the segments derived on the
199 piecewise regression to the sound wood threshold using a lower-tailed z-test (alpha = 0.05, Flores-
200 Moreno et al., 2024). From this we determined the total proportion of damage on the linear transect
201 captured by the residrill trace (see Flores-Moreno et al., 2024 for data processing details). Proportion
202 damage was estimated on a linear basis on the assumption that damage accumulates randomly. To
203 quantify the absolute amount of internal damage, we calculated the total undamaged area (cm²) of the
204 cross section of the tree stem at each measurement point using the area of a circle = $\pi(d/2)^2$ (d is stem
205 diameter at the height of measurement). We then multiplied the undamaged area by the damage
206 proportion to derive the total damaged area (cm²).

207

208 *Calculating damage in the main stem using a single-sample estimate: constant damage*

209 We modeled the segment of lower stem sampled with the residrill (50-180 cm from the ground) as a
210 truncated cone, or frustum (Figure 1). The frustum tapers linearly from bottom to top, reflecting the
211 tapering shape of tree stems. We calculated the volume of the undamaged frustum (representing a
212 segment of the lower tree stem) using the following equation (Larsen 2017):

213

$$214 \quad V = \frac{L}{3}(A_l + \sqrt{A_l A_s} + A_s)$$

215

216 Where V is volume of the lower stem, L is the length of the frustum, A_l is the area of the frustum bottom
217 (50 cm from the ground), and A_s is the area of the frustum top (180 cm from the ground).

218

219 To calculate damaged volume in the lower stem using a single-sample damage estimate, we multiplied the
220 undamaged frustum volume by the proportion of damage from the residrill measurement ~120 cm from
221 tree base. The 120 cm measurement allowed for comparison with methods from Flores-Moreno et al.
222 (2024), with the caveat that we used the closest measurement to DBH (1.2 m), since our sampling design
223 did not record internal damage exactly at 1.3 m from the ground (true DBH measurement). To convert
224 damaged volume to damaged biomass (in kg) in the lower stem, we multiplied the damaged volume from
225 the single-sample estimate by species-level wood density values (Supplementary Table 2).

226

227 *Calculating damage in the main stem using a multi-sample estimate: variable damage*

228 To calculate damaged volume in the lower stem using a multi-sample damage estimate, we defined a
229 tapering relationship for how damage changed between the bottom and top of the lower stem. We
230 modified the frustum equation from Larsen (2017) so that A_l and A_s represented the area of damage from
231 the lowest (50 cm) and highest measurements (180 cm) on the stem. We multiplied the damaged volume
232 by species-level wood density values to convert to biomass (kg).

233

234 *Assessing external damage pressures: termite presence and fire scarring*

235 Trees were inspected for external termite presence, defined as termite runways on the stem (Figure 3b) or
236 mounds built at the tree base (Figure 3c). Additionally, we recorded the presence or absence of moderate
237 to severe fire scarring, identified as damage to basal bark or charred surfaces covering at least 25% of the
238 lower stem (Figure 3d).

239

240 *Analyses*

241 *Internal stem damage variation with vertical position across tree species*

242 We tested how damage, both as an absolute amount (**H1**) and as a proportion (**H2**), changed with vertical
243 position and if this varied by tree species. To determine the relationship between proportion damage,
244 vertical position on the lower stem, and tree species, we used a beta regression model with a logit link
245 from the package glmmTMB (Brooks et al., 2017). Proportional stem damage was the response variable
246 and vertical position (i.e., residrill height from the ground, cm) and tree species were fixed effects, with
247 tree individual and site as random effects. A Tukey's Honest Significant Difference (HSD) pairwise post-
248 hoc multiple comparisons test was used to determine which species significantly differed.

249

250 To determine the relationship between absolute amount of damage, vertical position on the lower stem,
251 and species, we used a linear mixed effect model from the package lmer (Bates et al., 2015). In the model,
252 area of stem damage (cm²) was the log-transformed response (to meet the normality assumption) while
253 vertical position (cm) and tree species were fixed effects, and tree individual and site as random effects. A
254 Tukey's HSD pairwise post-hoc multiple comparisons test was used to determine which species
255 significantly differed.

256

257 *Internal stem damage variation with vertical position across tree traits (DBH and wood density)*

258 We tested if tree traits underlie species-level differences in vertical variation of both proportion and
259 absolute amount of internal stem damage. We use a beta regression model with a logit link where
260 proportion stem damage was the response variable, vertical position on the lower stem, DBH, and
261 species-level wood density were fixed effects, and tree individual and site as random effects. To test the
262 effect of tree traits on the absolute amount of damage, we used a linear mixed effect model where
263 damaged area was the log-transformed response variable (for normality) and vertical position, tree DBH,
264 and species-level wood density were fixed effects, with tree individual and site as random effects.

265

266 *Damaged biomass in the lower stem: comparing single-sample versus multi-sample methods*

267 We used a non-parametric paired Wilcoxon signed rank exact test (due to a non-normal distribution) to
268 determine if a single-sample estimate of total damaged biomass in the lower stem differed from a multi-
269 sample estimate.

270

271 *Differences in total damaged biomass by species, tree traits and presence of external damage pressures*

272 We first tested species-level differences in total damaged biomass in the lower stem (in kg) using a linear
273 mixed effects model with total damaged biomass as a response variable (log-transformed), species as a
274 fixed effect, and site as a random effect. A Tukey's HSD pairwise post-hoc multiple comparisons test was
275 used to determine which species were significantly different. To test if underlying tree traits explained
276 species-level differences, we ran a linear mixed effect model with total damaged biomass as a response
277 variable (log-transformed), tree DBH and species-level wood density as fixed effects, and site as a
278 random effect. We also ran an ANOVA to test for species-level differences in DBH, followed by a Tukey
279 HSD pairwise post-hoc test. Lastly, we tested if external damage pressures contributed to greater
280 damaged biomass using a linear mixed effect model where damaged biomass was the response (log-
281 transformed), external termite presence or fire scarring were fixed effects, and site as a random effect. We
282 also tested for an interaction between external termite presence or fire scarring.

283

284 *External damage pressure effects across tree species and traits*
285 We used a Fisher's exact test to determine if the presence or absence of external termite and fire scarring
286 differed across species. We prepared the data as counts of presence or absence of external termite and
287 external fire damage into separate contingency tables. Following a significant test result we used a
288 pairwise Fisher test as a post-hoc comparison with a False Discovery Rate (FDR) test to correct p-values
289 for multiple comparisons. Then, we tested the role of tree traits (DBH and species-level wood density) in
290 influencing external damage pressures (presence/absence) using a binomial model with a logit link. When
291 DBH and wood density were included as predictors in a combined model, collinearity was high. For this
292 reason, we ran separate binomial models testing each tree trait (DBH, wood density) against external
293 termite presence and fire scarring. All analyses were performed in R 4.4.1 (R Core Team, 2024).
294

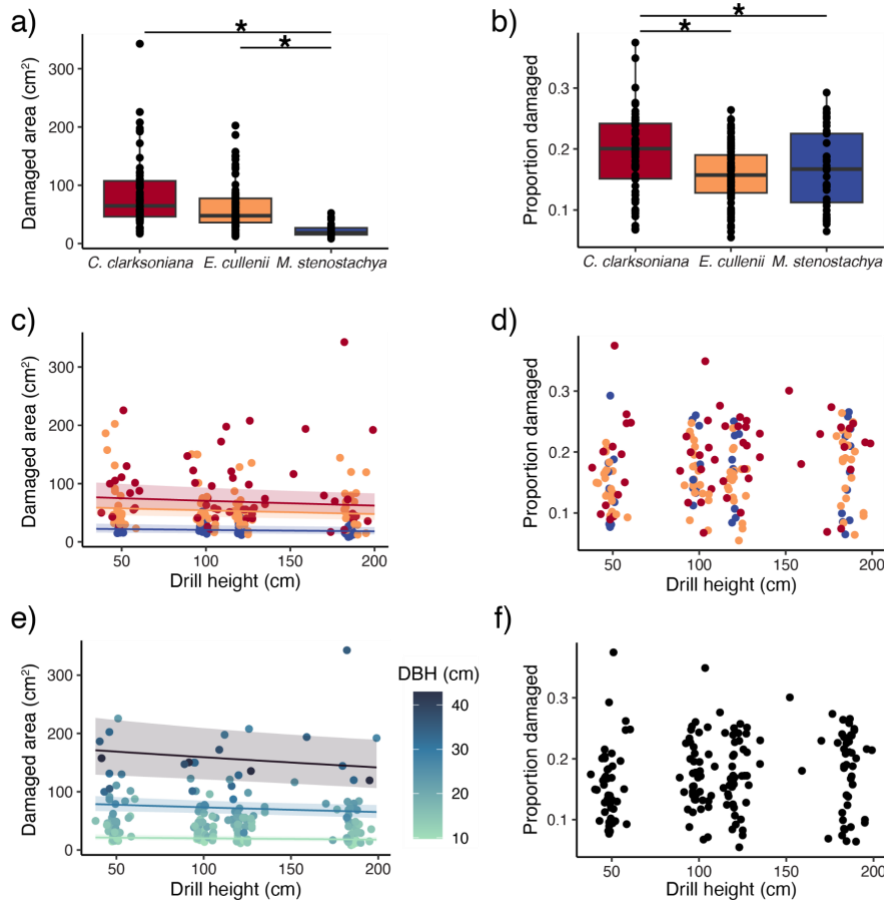
295 **Results**

296 *Internal stem damage variation with vertical position across tree species*

297 The absolute amount of internal stem damage varied by species ($p < 0.001$, Figure 4a) and decreased with
298 higher vertical position on the stem ($p = 0.01$, Figure 4c). Proportional damage varied by species ($p =$
299 0.001 , Figure 4b) but did not change with vertical position on the main stem ($p = 0.09$, Figure 4d,
300 Supplementary Table 3).
301

302 *Internal stem damage variation with vertical position across tree traits (DBH and wood density)*

303 Damaged area increased for trees with larger DBH ($p < 0.001$) and decreased at higher vertical positions
304 on the lower stem ($p = 0.02$, Figure 4e). Wood density did not affect the amount of damaged area ($p =$
305 0.70). Proportion damage did not significantly change across tree DBH, wood density, or vertical position
306 on the lower stem (Figure 4f, Supplementary Table 4).



307
 308 Figure 4. Species-level differences in a) absolute amount and b) proportion stem damage. Species-level
 309 differences for c) absolute amount of damage and d) proportion damage for vertical positions (cm from
 310 ground). Colors in c) and d) represent tree species indicated in a) and b). Tree traits that significantly
 311 affect e) absolute amount of damage and f) proportion damage at different vertical stem positions. Colors
 312 in e) indicate three selected DBH values capturing small, medium, and large trees respective to our
 313 dataset (purple = 34 cm, blue = 25 cm, green = 10 cm). Shading represents 95% confidence intervals.

314

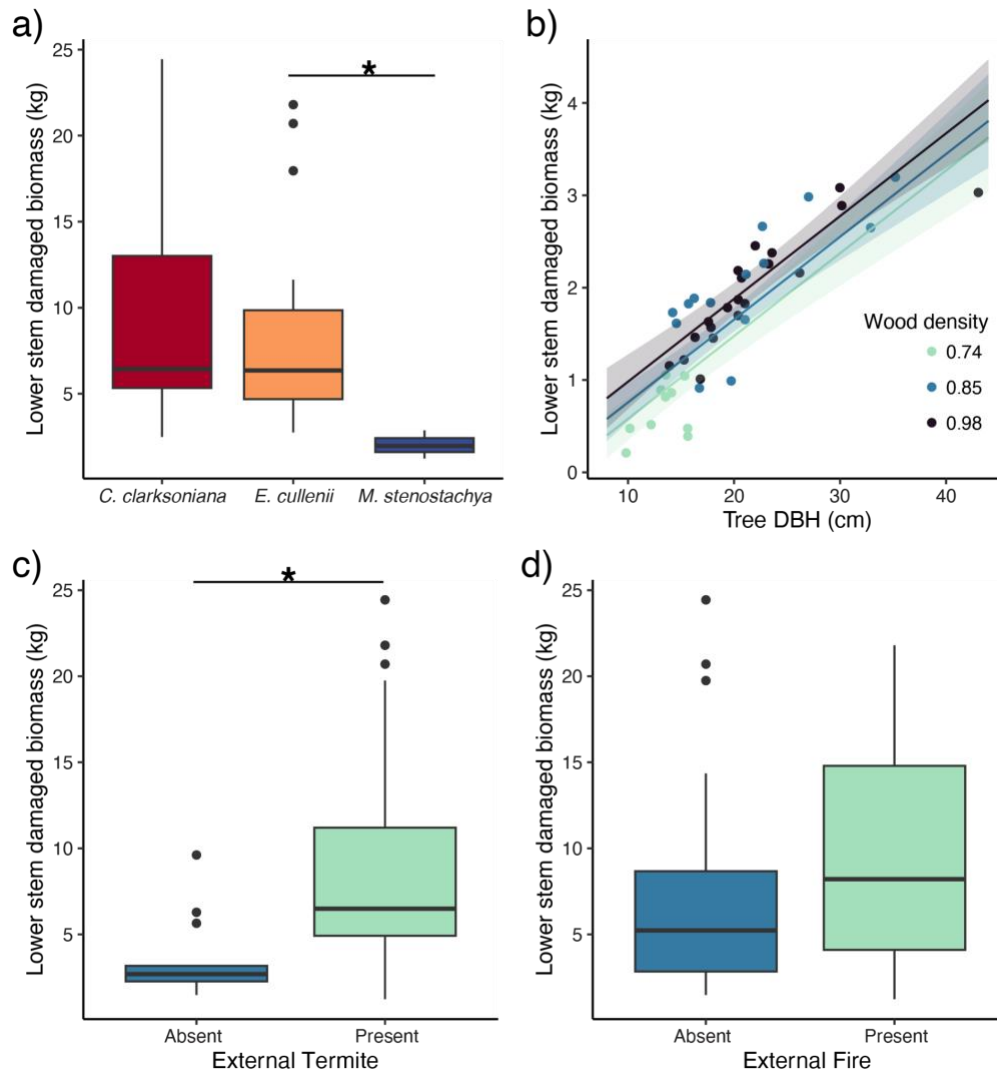
315 *Damaged biomass in the lower stem: comparing single-sample versus multi-sample methods*

316 There was no difference in the amount of damaged biomass when assuming constant damage (single-
 317 sample) or variable damage (multi-sample) ($p = 0.75$, Supplementary Figure 2).

318

319 *Differences in total damaged biomass by species, tree traits and presence of external damage*
 320 *pressures*

321 Total lower stem internal damage varied by species ($p < 0.001$). *E. cullenii* trees had significantly higher
 322 damage than *M. stenostachya* trees ($p < 0.0001$, Figure 5a). Larger ($p < 0.001$) and densely-wooded ($p =$
 323 0.01) trees had more total damaged biomass (Figure 5b). Species significantly differed in DBH
 324 (Supplementary Table 5); *E. cullenii* and *C. clarksoniana* trees were larger than *M. stenostachya*
 325 (Supplementary Figure 3). Total damaged biomass was higher for trees with external termite presence (p
 326 < 0.001 , Figure 5c), but not fire scarring ($p = 0.30$, Figure 5d).



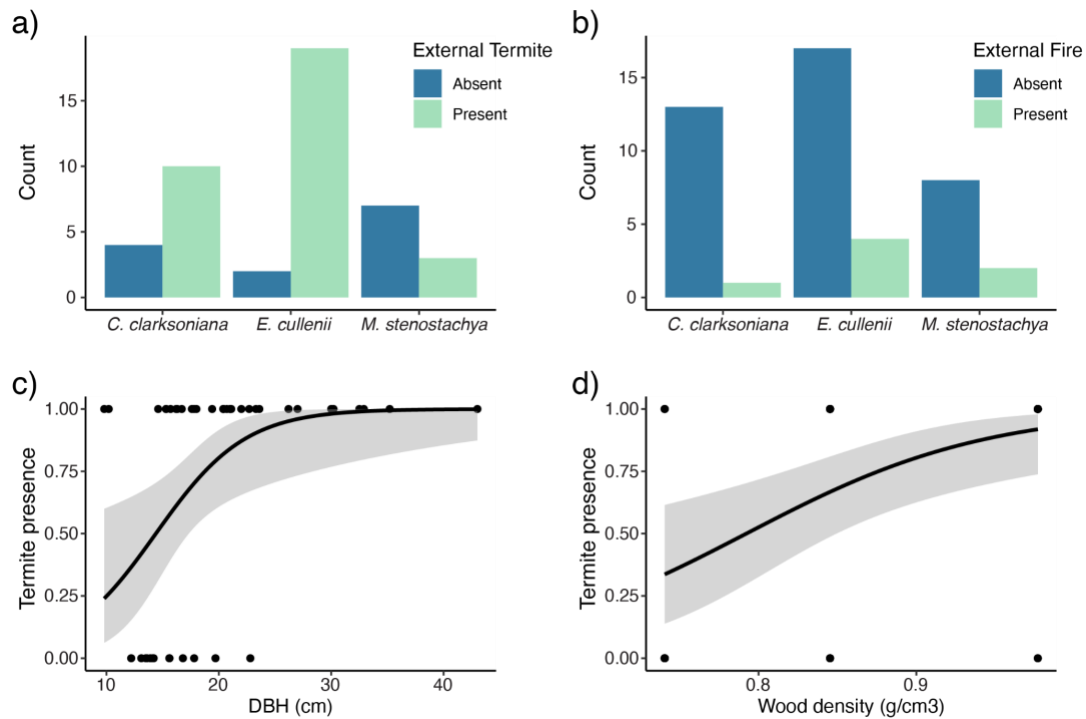
327
 328 Figure 5. Total damaged biomass (kg) in the lower stem for a) different species, b) DBH and wood
 329 densities, c) external termite presence/absence, and d) external fire scarring presence/absence.

330

331 *External damage pressure effects across tree species and traits*

332 Species differed in how external termite presence predicted internal damage ($p = 0.003$), with significant
 333 differences between *E. cullenii* and *M. stenostachya* trees ($p = 0.01$, Figure 6a). There was no significant
 334 difference between species in how the presence of external fire scarring predicted damage ($p = 0.65$,
 335 Figure 6b). External termite presence increased with tree DBH ($p = 0.001$, Figure 6c) and wood density (p
 336 < 0.001 , Figure 6d), but external fire scarring on the stem was not predicted by tree DBH ($p = 0.79$) or
 337 wood density ($p = 0.83$).

338



339
 340 Figure 6. a) External termite presence/absence and b) external fire scarring presence/absence for the three
 341 study species. Relationship between trees with external termite presence and c) tree DBH and d) wood
 342 density. Shaded areas represent 95% confidence intervals.

343
 344 **Discussion**

345 In this study, we examined vertical variation of internal stem damage and tested how species, tree traits,
 346 and external damage pressures contributed to internal stem damage. The absolute amount of internal stem
 347 damage decreased with higher vertical position on the stem, supporting **H1**, the ‘damage at the base’
 348 hypothesis. The amount of damage varied by species, which was likely due to the underlying influence of
 349 stem size. Proportion damage remained constant in the lower stem and no differences were found between
 350 single and multiple point estimates of total damage, supporting **H2**, the ‘strong home’ hypothesis. Total
 351 damage in the lower stem varied by species likely due to differences in tree DBH and wood density;
 352 external termite presence was also associated with increased total damaged biomass. Furthermore,
 353 external termite presence varied by tree species and occurred more frequently in large, dense trees. Below
 354 we discuss the implications of our findings on modeling internal stem damage and propose that
 355 understanding the specific role of termites can help address uncertainties in tree carbon estimates beyond
 356 savanna ecosystems.

357
 358 *Amount of internal damage decreased with increasing vertical position on the lower stem*

359 The decline in the absolute amount of damage with height supports the ‘damage at the base’ hypothesis
 360 (**H1**) and indicates a biophysical constraint where damage accumulation was dictated by the amount of
 361 wood at any given point on the stem. Due to tree taper, stem size decreases from the base to crown
 362 branches (McTague & Weiskittel 2021). Therefore, more wood is available for consumption at the lowest
 363 point of measurement (50 cm from the ground) compared to the highest point (180 cm) from the ground.
 364 Our models showed that larger trees had greater internal damage, further supporting that there is a

365 biophysical constraint on damage accumulation, since these trees hold more biomass. The presence of
366 damage pressures (termites and fire scarring) often coincides with where wood resources are highest: at
367 the tree base (Li et al., 2016; N'Dri et al., 2011). Therefore the tree base serves as an access point for
368 decomposers (Adkins 2006) and area where damage is concentrated.

369
370 Our results also support the ‘strong home’ hypothesis (**H2**), as proportional internal stem damage did not
371 change through the lower stem. This supports the key assumption used in Flores-Moreno et al. (2024) for
372 estimating internal stem damage: a single proportion was used to represent damage incurred by the whole
373 tree, which was then applied to scale internally damaged biomass to the plot-level. Tree hollowing from
374 termites (Werner & Prior 2007) is likely responsible for the constant damage proportion, as termites are
375 the main wood decomposer at the study sites (Clement et al., 2021; Flores-Moreno et al., 2024). Tree
376 hollowing termites often reside in the cavities they create (Greaves 1962). It may be strategic for termites
377 to remove wood in a constant proportion, as the tree structure can still maintain stability if hollowing does
378 not exceed 70% of the trunk radius (Mattheck et al., 2006).

379
380 However, it remains critical to quantify vertical variation in internal stem damage in other locations with
381 and without strong termite decomposition pressures, such as other savannas as well as non-savanna
382 ecosystems. In contrast to our findings, in a higher rainfall savanna ecosystem in Australia, Calvert et al.
383 (2024) showed a decreasing pattern in internal damage. This ecosystem had strong internal decomposition
384 pressures from both termites and microbes (Yatsko et al., 2024), and damage was modeled using samples
385 from the main stem and crown branches. While the present study does not show the same decreasing
386 trend, variation in both the strength of termite decomposition pressure and environmental conditions (i.e.,
387 rainfall) could explain the differences. Rainfall may be important for predicting the relative strength of
388 termites versus microbes as internal decomposers, which could alter patterns of damage through the tree.
389 Flores-Moreno et al. (2024) showed that rainforest trees had less internal stem damage than savanna trees
390 but could not identify how each process was influenced by different decomposers. Yet, it is known in
391 downed deadwood that microbial decay played a greater role in tropical wet rainforest wood
392 decomposition compared to savanna sites (Wijas, Flores-Moreno et al., 2024). Therefore, if microbial
393 decay dominates internal stem damage, vertical variation may present differently than what was observed
394 here for savanna trees, making the ‘strong home’ hypothesis less applicable. Since many accounts of
395 microbial heartrot in both temperate and tropical trees have been noted (Frank et al., 2018; Lee et al.,
396 1988; Heineman et al., 2015), efforts to sample stem damage vertical variation in such environments are
397 required to determine if the patterns in this study can be generalized.

398
399 *Damage across species, tree traits, and wood characteristics*

400 We detected differences in species-level damage accumulation, with *C. clarksoniana* trees being most
401 damaged and *M. stenostachya* least. Cross-species differences were most strongly driven by stem size,
402 wood density, and external termite presence, however the broad shift in damage across species occurred
403 at the overall amount of damage (i.e., intercept) but not in the accumulation of damage across the stem
404 (i.e., slope). From this, we draw two main conclusions: 1) wood characteristics at the species-level are
405 important controls on how much wood is consumed (i.e., explaining species differences in intercepts), and
406 2) across species, there may be a general relationship between internal damage accumulation and height
407 (i.e., consistency of slopes across species). A closer evaluation of other physical and chemical wood
408 properties that may improve palatability for decomposers is a necessary next step. For example, termites

409 consider factors other than wood density and resource size in foraging decisions, such as the early wood
410 content (lighter colored, less dense wood), moisture levels, and even how well the substrate serves as a
411 communication medium (Oberst et al., 2018). Such factors could be quantified using termite choice
412 experiments to test for species-level differences in wood palatability. Following the second conclusion,
413 we propose that if patterns of internal damage are generalizable across species or environments, they
414 could be easily integrated into biomass models by assuming a constant slope. This would be an important
415 next step toward incorporating internal stem damage into AGB accounting, which has yet to be
416 accomplished (Flores-Moreno et al., 2024; Calvert et al., 2024). Yet it remains essential to test whether
417 the patterns we find here extend to other ecosystem types and species to best inform AGB models more
418 broadly.

419
420 Interestingly, both this study and Calvert et al. (2024) found 20% internal stem damage in *Corymbia*
421 *clarksoniana* trees at two different savanna sites 600 km apart, despite variations in annual rainfall. This
422 consistency suggests a potential pattern, but more sampling across different locations is essential to
423 confirm whether this trend holds. To our knowledge, no studies have compared internal stem damage
424 within species across sites, but such data will be invaluable in documenting the robustness of patterns on
425 species-specific internal stem damage. Expanding data collection efforts to measure internal stem damage
426 at the species-level across geographic and size ranges could directly feed into novel AGB models built to
427 incorporate the effect of internal stem damage. A comprehensive database of species-level damage and
428 vertical variation would greatly improve our understanding of missing biomass across ecosystems.

429
430 *A home for termites inside of trees: contributing factors and global extent*
431 The role of wood density and stem size in predicting internal damage goes hand in hand with **H1** and **H2**,
432 where termites are targeting trees that can provide large, strong homes. For example, *C. clarksoniana*
433 trees had the greatest amount of internal damage in the lower stem, which is reflected in their high density
434 wood (0.85 g/cm³) and generally larger stem size. Dense wood and large stem size provides strength to
435 the tree structure (Larjavaara & Muller-Landau 2010), and since damage has not passed a critical
436 breakage threshold of 70% (Mattheck et al., 2006), the tree remains structurally uncompromised and
437 forms a well-protected hollow. Here, we tested a limited range of wood densities (0.7-0.9 g/cm³) and
438 DBH values (10-43 cm), yet the general patterns remain congruent with Flores-Moreno et al. (2024), who
439 showed moderate strength of wood density and DBH as predictors of internal damage across a broader
440 range of values (wood density: 0.4-0.9 g/cm³, DBH: 10-125 cm).

441
442 Studies in north Australian savannas have shown that dense-wooded Myrtaceae trees (including
443 *Corymbia* and *Eucalyptus*) are often hollowed by *Coptotermes* termites (Greaves 1962, Perry et al., 1985,
444 Werner & Prior 2007). These trees dominate the species diversity in Australian savannas (Crisp & Cook
445 2013) and quantifying the extent of internal damage in these trees across the continent will improve AGB
446 estimation at landscape scales (Calvert et al., 2024). While tree hollowing has been most extensively
447 described in Australian savannas, it remains an open question if these patterns hold in other Australian
448 ecosystems or other parts of the globe where wood nesting termites are present. Termite-derived internal
449 stem damage has been reported in other ecosystems, such as *Coptotermes* species in the Brazilian
450 Amazon described to colonize heartwood of living trees (Eleuterio et al., 2020). In southeastern Florida,
451 USA, an invasive pest species, *C. gestroi*, threatens the urban tree canopy by causing extensive damage in
452 numerous tree species (Chouvenc & Foley 2018). Also, *C. formosanus* in Louisiana, USA infest and

453 internally damage multiple species of urban trees (Osbrink et al., 1999). *C. gestroi* and *C. formosanus* are
454 highly invasive species with global distributions (GBIF 2024), providing a strong case for future efforts to
455 quantify internal stem damage extent more thoroughly outside of Australian savannas.

456

457 *Linking external damage to internal damage*

458 While internal damage is concealed within trees and therefore challenging to detect without invasive
459 measurements, we find that external termite presence can indicate what is happening inside trees. One
460 caveat is that it is not entirely possible to confirm termites as the direct cause without examining the
461 interior wood (Yatsko et al., 2024). Yet, links between external and internal damage have also been
462 demonstrated by Flores-Moreno et al. (2024), where authors found a strong positive relationship between
463 the activity of termites in surrounding deadwood and internal stem damage, especially for densely-
464 wooded savanna trees. Other studies in northern Australia related increased termite activity with greater
465 numbers of tree hollows (Woinarski & Westaway 2008; Woolley et al., 2018) and indicated termites,
466 particularly those of the genus *Coptotermes*, as agents of internal damage (Greaves 1962; Werner & Prior
467 2007; Yatsko et al., 2024). However, it is not enough to rely only on termite presence; knowing which
468 species are present is critical. For example, *Nasutitermes graveolus*, an arboreal-nesting species common
469 to our study area creates external runways on tree stems but is not known to forage in crown or stem
470 wood. Rather, *N. graveolus* uses the runways for protection as they transit to reach deadwood on the
471 ground (Hill 1942). In contrast, *C. acinaciformis* often build mounds at the tree base and then feed on
472 internal tree wood (Yatsko et al., 2024). Most termites that we found associated with sampled stems were
473 *C. acinaciformis*. *N. graveolus* was present to a lesser extent, and a *Microcerotermes* species was also
474 found, which has not been widely associated with internal wood decomposition. Overall, external termite
475 presence can indicate greater internal tree hollowing, but it is necessary to consider which species are
476 present.

477

478 We did not observe increased internal damage for trees with basal fire scarring as expected; internal stem
479 damage can be facilitated by fire, which creates conditions for further biotic colonization (N'Dri et al.,
480 2011). In our system, external fire damage may not indicate greater internal stem damage due to fire
481 severity. N'Dri et al. (2011) found more frequent basal openings in trees exposed to higher severity fires,
482 yet the region of our study site is managed with low-severity fires through early dry-season burning.
483 Therefore, lower fire intensity may not result in suitable basal scarring that promotes biotic invasion.
484 Furthermore, external fire damage did not vary across tree species or sizes, suggesting that its influence is
485 not mediated by selection of tree traits, at least for the species considered here.

486

487 *Incorporating internal stem damage into estimates of tree carbon*

488 Accurate estimation of carbon sequestered in trees is necessary for validating nature-based climate change
489 solutions and forest carbon markets (Chave et al., 2014). In this study among a few others (Flores-Moreno
490 et al., 2024, Calvert et al., 2024), we demonstrate that internal stem damage removes tree AGB in the
491 lower stem, with consequences for reducing aboveground carbon storage. It is necessary for future studies
492 to broaden internal damage sampling to other forest types and locations, especially to capture damage in
493 the main stem where a large proportion of total tree biomass is held (Ribeiro et al., 2015). Additionally,
494 little is known about crown branch damage due to sampling difficulty; it will be important to characterize
495 the amount of damage and the role of microbes and termites in these structures. Consideration should also
496 be paid to large, dense trees that contain high biomass on the landscape for long time periods (Stephenson

497 et al., 2014; Lutz et al., 2018). Indeed, Calvert et al. (2024) showed how unaccounted for damage in such
498 trees can result in consequential biomass overestimation, demonstrating that even with the use of high-
499 accuracy biomass estimation (e.g., terrestrial laser scanning), internal damage cannot be captured,
500 inevitably resulting in biomass overestimates.

501
502 Current internal stem damage sampling efforts remain quite sparse and efforts to extend measurements to
503 new species and ecosystems will determine the generalizability of the patterns observed in the present
504 study. The following practices will help to overcome current limitations in incorporating internal stem
505 damage into AGB estimation for the world's forests: Where termites are prominent wood decomposers, it
506 should be a priority to survey trees for external termite presence, as this can indicate where hollowing
507 may take place. Widespread characterization of internal damage (i.e., using a residrill at DBH) in other
508 termite-dominated systems will help to determine the extent of this phenomenon. Focused sampling on
509 large, dense trees is key as these are large carbon reservoirs. Lastly, future research should test if tree
510 hollowing is a *Coptotermes* genus-wide behavior, and target internal damage sampling in regions where
511 *Coptotermes* occurs, either naturally or as an invasive species. Prioritizing these efforts and increasing the
512 global coverage of internal stem damage sampling will provide clearer insights into its ecological impact
513 and help refine forest biomass and carbon accounting.

514

515 **Acknowledgements**

516 We thank Lucas Cernusak for allowing us to use lab space at James Cook University Cairns for the
517 duration of this project and we thank Alex Cheesman for assistance with fieldwork logistics. We are
518 grateful for support in the field from Kerri and Gavin Enever, the station managers at the Brooklyn
519 Sanctuary, and to the Australian Wildlife Conservancy for allowing us to sample at their property.

520

521 **Author contribution**

522 Abbey R. Yatsko, Habacuc Flores-Moreno, and Amy E. Zanne conceived the ideas and designed
523 methodology; Abbey R. Yatsko and Michaela Fitzgerald collected the data; Abbey R. Yatsko and
524 Habacuc Flores-Moreno analyzed the data; Abbey R. Yatsko led the writing of the manuscript. All
525 authors contributed to manuscript editing and review and gave final approval for publication.

526

527 **Data availability statement**

528 We intend to archive the data for this study at Zenodo through the Zanne Lab, University of Miami.
529 Specific DOIs will be provided once data is uploaded.

530

531 **Statement on inclusion**

532 This study is a collaboration between researchers from the USA and Australia, and all members were
533 involved in the conceptualization and data collection process. We cite regionally relevant literature when
534 available in our manuscript.

535

536 **Conflicts of interest**

537 The authors declare no conflicts of interest.

538

539 **References**

- 540 Adkins, M.F. (2006). A burning issue: Using fire to accelerate tree hollow formation in Eucalyptus
 541 species. *Australian Forestry*, 69(2), 107–113. <https://doi.org/10.1080/00049158.2006.10676236>
 542 Bates, D., Mächler, M., Bolker, B., & Walker, S. (2015). Fitting Linear Mixed-Effects Models Using
 543 lme4. *J. Stat. Softw.*, 67, 1–48. <https://doi.org/10.18637/jss.v067.i01>
 544 Brooks, M. E., Kristensen, K., van Benthem, K.J., Magnusson, A., Berg, C.W., Nielsen, A., Skaug,
 545 H.J., Machler, M., & Bolker, B.M. (2017). glmmTMB balances speed and flexibility among
 546 packages for zero-inflated generalized linear mixed modeling. *The R Journal*, 9(2), 378–400.
 547 <https://doi.org/10.3929/ethz-b-000240890>
 548 Brown, I.F., Martinelli, L.A., Thomas, W.W., Moreira, M.Z., Cid Ferreira, C.A., & Victoria, R.A.
 549 (1995). Uncertainty in the biomass of Amazonian forests: An example from Rondônia, Brazil.
 550 *For. Ecol. Manag.*, 75(1–3), 175–189. [https://doi.org/10.1016/0378-1127\(94\)03512-U](https://doi.org/10.1016/0378-1127(94)03512-U)
 551 Calvert, J., Yatsko, A.R., Bresgi, J., Cheesman, A.W., Cook, K., Crowe, J., Gambold, I., Jones, C.,
 552 O’Connor, L., Peter, T., Russell-Smith, P., Taylor, E., Trigger, B., Wijas, B., & Zanne, A.E.
 553 (2024). Modelling internal stem damage in savanna trees: Error in aboveground biomass with
 554 terrestrial laser scanning and allometry. *Methods Ecol. Evol.*, 2041-210X.14375.
 555 <https://doi.org/10.1111/2041-210X.14375>
 556 Chave, J., Réjou-Méchain, M., Búrquez, A., Chidumayo, E., Colgan, M.S., Delitti, W.B.C., Duque,
 557 A., Eid, T., Fearnside, P.M., Goodman, R.C., Henry, M., Martínez-Yrizar, A., Mugasha, W.A.,
 558 Muller-Landau, H.C., Mencuccini, M., Nelson, B.W., Ngomanda, A., Nogueira, E.M., Ortiz-
 559 Malavassi, ... Vieilledent, G. (2014). Improved allometric models to estimate the aboveground
 560 biomass of tropical trees. *Glob. Change Biol.*, 20: 3177-3190.
 561 <https://doi.org/10.1111/gcb.12629>
 562 Cheesman, A.W., Cernusak, L.A., & Zanne, A.E. (2018). Relative roles of termites and saprotrophic
 563 microbes as drivers of wood decay: A wood block test. *Austral Ecology*, 43(3), 257–267.
 564 <https://doi.org/10.1111/aec.12561>
 565 Chouvenc, T., & Foley, J.R. (2018). Coptotermes gestro (Wasmann) (Blattodea [Isoptera]:
 566 Rhinotermitidae), a Threat to the Southeastern Florida Urban Tree Canopy. *Florida*
 567 *Entomologist*, 101(1), 79–90. <https://doi.org/10.1653/024.101.0115>
 568 Clement, R.A., Flores-Moreno, H., Cernusak, L.A., Cheesman, A.W., Yatsko, A.R., Allison, S.D.,
 569 Eggleton, P., & Zanne, A.E. (2021). Assessing the Australian Termite Diversity Anomaly: How
 570 Habitat and Rainfall Affect Termite Assemblages. *Front. Ecol. Evol.*, 9, 657444.
 571 <https://doi.org/10.3389/fevo.2021.657444>
 572 Climent, J., Chambel, M.R., Gil, L., & Pardos, J.A. (2003). Vertical heartwood variation patterns
 573 and prediction of heartwood volume in Pinus canariensis Sm. *For. Ecol. Manag.*, 174(1–3),
 574 203–211. [https://doi.org/10.1016/S0378-1127\(02\)00023-3](https://doi.org/10.1016/S0378-1127(02)00023-3)
 575 Crisp, M.D., & Cook, L.G. (2013). How Was the Australian Flora Assembled Over the Last 65
 576 Million Years? A Molecular Phylogenetic Perspective. *Annu. Rev. Ecol. Evol. Syst.*, 44(1), 303–
 577 324. <https://doi.org/10.1146/annurev-ecolsys-110512-135910>
 578 Dobson, A., Hopcraft, G., Mduma, S., Ogotu, J.O., Fryxell, J., Anderson, T.M., Archibald, S.,
 579 Lehmann, C., Poole, J., Caro, T., Mulder, M.B., Holt, R.D., Berger, J., Rubenstein, D.I.,
 580 Kahumbu, P., Chidumayo, E.N., Milner-Gulland, E.J., Schluter, D., Otto, S., ... Sinclair, A.R.E.
 581 (2022). Savannas are vital but overlooked carbon sinks. *Science*, 375(6579), 392–392.
 582 <https://doi.org/10.1126/science.abn4482>
 583 Eleuterio, A.A., de Jesus, M.A., & Putz, F.E. (2020). Stem decay in live trees: Heartwood hollows
 584 and termites in five timber species in eastern Amazonia. *Forests*, 11(10), 1–12.
 585 <https://doi.org/10.3390/f11101087>
 586 Flores-Moreno, H., Yatsko, A.R., Cheesman, A.W., Allison, S.D., Cernusak, L.A., Cheney, R.,
 587 Clement, R.A., Cooper, W., Eggleton, P., Jensen, R., Rosenfield, M., & Zanne, A.E. (2024).

588 Shifts in internal stem damage along a tropical precipitation gradient and implications for forest
589 biomass estimation. *New Phytol.*, 241(3), 1047–1061. <https://doi.org/10.1111/nph.19417>

590 Frank, J., Castle, M.E., Westfall, J.A., Weiskittel, A.R., Macfarlane, D.W., Baral, S.K., Radtke, P. .,
591 & Pelletier, G. (2018). Variation in occurrence and extent of internal stem decay in standing
592 trees across the eastern US and Canada: Evaluation of alternative modelling approaches and
593 influential factors. *Forestry*, 91(3), 382–399. <https://doi.org/10.1093/forestry/cpx054>

594 GBIF.org (16 August 2024) GBIF Occurrence Download <https://doi.org/10.15468/dl.uf46um>

595 Gilbert, G.S., Ballesteros, J.O., Barrios-Rodriguez, C.A., Bonadies, E.F., Cedeño-Sánchez, M.L.,
596 Fossatti-Caballero, N.J., Trejos-Rodríguez, M.M., Pérez-Suñiga, J.M., Holub-Young, K.S.,
597 Henn, L.A.W., Thompson, J.B., García-López, C.G., Romo, A.C., Johnston, D.C., Barrick,
598 P.P., Jordan, F.A., Hershovich, S., Russo, N., Sánchez, J.D., ... Hubbell, S.P. (2016). Use of
599 sonic tomography to detect and quantify wood decay in living trees. *Appl. Plant Sci.*, 4(12),
600 1600060–1600060. <https://doi.org/10.3732/apps.1600060>

601 Grace, J., José, J.S., Meir, P., Miranda, H.S., & Montes, R.A. (2006). Productivity and carbon fluxes
602 of tropical savannas. *J. Biogeogr.*, 33(3), 387–400. <https://doi.org/10.1111/j.1365-2699.2005.01448.x>

603

604 Greaves, T. (1962). Studies of foraging galleries and the invasion of living trees by *Coptotermes*
605 *acinaciformis* and *C. Brunneus* (Isoptera). *Aust. J. Zool.*, 10(4), 630–651.
606 <https://doi.org/10.1071/ZO9620630>

607 Harja, D., Rahayu, S., & Pambudi, S. 2019. Tree functional attributes and ecological database.
608 <http://db.worldagroforestry.org/> [accessed 12 February 2024].

609 Heineman, K.D., Russo, S.E., Baillie, I.C., Mamit, J.D., Chai, P.P.K., Chai, L., Hindley, E.W., Lau,
610 B.T., Tan, S., & Ashton, P.S. (2015). Evaluation of stem rot in 339 Bornean tree species:
611 Implications of size, taxonomy, and soil-related variation for aboveground biomass estimates.
612 *Biogeosciences*, 12(19), 5735–5751. <https://doi.org/10.5194/bg-12-5735-2015>

613 Hill, G. F. (1942). Termites (Isoptera) from the Australian region. 479-pp.
614 <https://www.cabdirect.org/cabdirect/abstract/19420602503>

615 Janzen, D. H. (1976). Why Tropical Trees Have Rotten Cores. *Biotropica*, 8(2), 110–110.

616 Larjavaara, M., & Muller-Landau, H.C. (2010). Rethinking the value of high wood density.
617 *Functional Ecology*, 24(4), 701–705. <https://doi.org/10.1111/j.1365-2435.2010.01698.x>

618 Larsen, D.R. (2017). Simple taper: Taper equations for the field forester. In: Kabrick, J.M. et al. eds.
619 *Proceedings of the 20th Central Hardwood Forest Conference* 265–278.
620 <https://research.fs.usda.gov/treesearch/53782>

621 Law, S., Flores-Moreno, H., Cheesman, A.W., Clement, R., Rosenfield, M., Yatsko, A., Cernusak,
622 L. A., Dalling, J.W., Canam, T., Iqsayya, I.A., Duan, E.S., Allison, S.D., Eggleton, P., & Zanne,
623 A.E. (2023). Wood traits explain microbial but not termite-driven decay in Australian tropical
624 rainforest and savanna. *J. Ecol.*, 111, 982–993. <https://doi.org/10.1111/1365-2745.14090>

625 Lee, S.S., Teng, S.Y., Lim, M.T., & Kader, R.A. (1988). Discolouration and heart rot of *Acacia*
626 *Mangium* Willd. - Some preliminary results. *J. Trop. For. Sci.*, 1(2), 170–177.
627 <http://www.jstor.org/stable/43594303>.

628 Li, H.F., Yeh, H.T., Chiu, C.I., Kuo, C.Y., & Tsai, M.J. (2016). Vertical distribution of termites on
629 trees in two forest landscapes in Taiwan. *Environmental Entomology*, 45(3), 577–581.
630 <https://doi.org/10.1093/ee/nvw019>

631 Lutz, J.A., Furniss, T.J., Johnson, D.J., Davies, S.J., Allen, D., Alonso, A., Anderson-Teixeira, K.J.,
632 Andrade, A., Baltzer, J., Becker, K.M.L., Blomdahl, E.M., Bourg, N.A., Bunyavejchewin, S.,
633 Burslem, D.F.R.P., Cansler, C.A., Cao, K., Cao, M., Cárdenas, D., Chang, L., ... Zimmerman,
634 J.K. (2018). Global importance of large-diameter trees. *Glob. Ecol. Biogeogr.*, 27(7), 849–864.
635 <https://doi.org/10.1111/geb.12747>

636 Mattheck, C., Bethge, K., & Tesari, I. (2006). Shear effects on failure of hollow trees. *Trees*, 20(3),
637 329–333. <https://doi.org/10.1007/s00468-005-0044-0>

638 Mattheck, C., Bethge, K., & West, P. . (1994). Breakage of hollow tree stems. *Trees*, 9(1).
639 <https://doi.org/10.1007/BF00197869>

640 McTague, J.P., & Weiskittel, A. (2021). Evolution, history, and use of stem taper equations: A
641 review of their development, application, and implementation. *Can. J. For. Res.*, 51(2), 210–
642 235. <https://doi.org/10.1139/cjfr-2020-0326>

643 Murphy, B.P., Whitehead, P.J., Evans, J., Yates, C.P., Edwards, A.C., MacDermott, H.J., Lynch,
644 D.C., & Russell-Smith, J. (2023). Using a demographic model to project the long-term effects
645 of fire management on tree biomass in Australian savannas. *Ecological Monographs*, 93(2),
646 e1564. <https://doi.org/10.1002/ecm.1564>

647 N’Dri, A.B., Gignoux, J., Konaté, S., Dembélé, A., & Aïdara, D. (2011). Origin of trunk damage in
648 West African savanna trees: The interaction of fire and termites. *J. Trop. Ecol.*, 27(3), 269–278.
649 <https://doi.org/10.1017/S026646741000074X>

650 Nogueira, E.M., Nelson, B.W., & Fearnside, P.M. (2006). Volume and biomass of trees in central
651 Amazonia: Influence of irregularly shaped and hollow trunks. *For. Ecol. Manag.*, 227(1–2),
652 14–21. <https://doi.org/10.1016/j.foreco.2006.02.004>

653 Oberst, S., Lai, J.C.S., & Evans, T.A. (2018). Key physical wood properties in termite foraging
654 decisions. *J. R. Soc. Interface.*, 15(149). <https://doi.org/10.1098/rsif.2018.0505>

655 Osazuwa-Peters, O.L., Wright, S.J., & Zanne, A.E. (2014). Radial variation in wood specific gravity
656 of tropical tree species differing in growth–mortality strategies. *Am. J. Bot.*, 101(5), 803–811.
657 <https://doi.org/10.3732/ajb.1400040>

658 Osbrink, Weste L.A., Woodson, W.D. & Lax, A.R. (1999). Population of Formosan subterranean
659 termite, *Coptotermes formosanus* (Isoptera: Rhinotermitidae), established in living urban trees
660 in New Orleans, Louisiana, USA. *3rd International Conference on Urban Pests*.

661 Parr, C.L., Lehmann, C.E.R., Bond, W.J., Hoffmann, W.A., & Andersen, A.N. (2014). Tropical
662 grassy biomes: Misunderstood, neglected, and under threat. *Trends Ecol. Evol.*, 29(4), 205–213.
663 <https://doi.org/10.1016/j.tree.2014.02.004>

664 Perry, D.H., Lenz, M., & Watson, J.A.L. (1985). Relationships between fire, fungal rots and termite
665 damage in Australian forest trees. *Australian Forestry*, 48(1), 46–53.
666 <https://doi.org/10.1080/00049158.1985.10674422>

667 R Core Team (2024). R: A language and environment for statistical computing. R Foundation for
668 Statistical Computing, Vienna, Austria. <https://www.R-project.org/>.

669 Ribeiro, S.C., Soares, C.P.B., Fehrmann, L., Jacovine, L.A.G., & Von Gadow, K. (2015).
670 Aboveground and belowground biomass and carbon estimates for clonal Eucalyptus trees in
671 southeast Brazil. *Revista Árvore*, 39(2), 353–363. [https://doi.org/10.1590/0100-](https://doi.org/10.1590/0100-67622015000200015)
672 [67622015000200015](https://doi.org/10.1590/0100-67622015000200015)

673 Scholes, R.J., & Archer, S.R. (1997). Tree-grass interactions in savannas. *Annu. Rev. Ecol. Syst.*, 28,
674 517–544. <https://doi.org/10.1146/annurev.ecolsys.28.1.517>.

675 Stephenson, N.L., Das, A.J., Condit, R., Russo, S.E., Baker, P.J., Beckman, N.G., Coomes, D.A.,
676 Lines, E.R., Morris, W.K., Rüger, N., Álvarez, E., Blundo, C., Bunyavejchewin, S., Chuyong,
677 G., Davies, S.J., Duque, A., Ewango, C.N., Flores, O., Franklin, J.F., ... Zavala, M.A. (2014).
678 Rate of tree carbon accumulation increases continuously with tree size. *Nature*, 507(7490), 90–
679 93. <https://doi.org/10.1038/nature12914>

680 Sullivan, M.J.P., Talbot, J., Lewis, S.L., Phillips, O.L., Qie, L., Begne, S.K., Chave, J., Cuni-
681 Sanchez, A., Hubau, W., Lopez-Gonzalez, G., Miles, L., Monteagudo-Mendoza, A., Sonké, B.,
682 Sunderland, T., ter Steege, H., White, L.J.T., Affum-Baffoe, K., Aiba, S., de Almeida, E.C., ...
683 Zemagho, L. (2017). Diversity and carbon storage across the tropical forest biome. *Scientific*
684 *Reports*, 7(1), Article 1. <https://doi.org/10.1038/srep39102>

685 Werner, P.A., & Prior, L.D. (2007). Tree-piping termites and growth and survival of host trees in
686 savanna woodland of north Australia. *J. Trop. Ecol.*, 23(6), 611–622.
687 <https://doi.org/10.1017/S0266467407004476>

688 Wijas, B., Allison, S., Austin, A., Cornwell, W., Cornelissen, J.H., Eggleton, P., Fraver, S., Ooi, M.,
689 Powell, J., Woodall, C., & Zanne, A. (2024). The role of deadwood in the carbon cycle:
690 Implications for models, forest management, and future climates. *Annu. Rev. Ecol. Evol. Syst.*
691 <https://doi.org/10.1146/annurev-ecolsys-110421-102327>
692 Wijas, B.J., Flores-Moreno, H., Allison, S.D., Rodriguez, L.C., Cheesman, A.W., Cernusak, L.A.,
693 Clement, R., Cornwell, W.K., Duan, E.S., Eggleton, P., Rosenfield, M.V., Yatsko, A.R., &
694 Zanne, A.E. (2024). Drivers of wood decay in tropical ecosystems: Termites versus microbes
695 along spatial, temporal and experimental precipitation gradients. *Functional Ecology*, 1365-
696 2435.14494. <https://doi.org/10.1111/1365-2435.14494>
697 Woinarski, J.C.Z., & Westaway, J. (2008). Hollow formation in the *Eucalyptus miniata* – E.
698 tetrodonta open forests and savanna woodlands of tropical northern Australia. Final report to
699 Land and Water Australia. Department of Natural Resources, Environment, Darwin.
700 Woolley, L.A., Murphy, B.P., Radford, I.J., Westaway, J., & Woinarski, J.C.Z. (2018). Cyclones,
701 fire, and termites: The drivers of tree hollow abundance in northern Australia’s mesic tropical
702 savanna. *For. Ecol. Manag.*, 419–420, 146–159. <https://doi.org/10.1016/j.foreco.2018.03.034>
703 Yatsko, A.R., Wijas, B., Calvert, J., Cheesman, A., Cook, K., Eggleton, P., Gambold, I., Jones, C.,
704 Russell-Smith, P., & Zanne, A.E. (2024). Why are trees hollow? Termites, microbes, and tree
705 internal stem damage in a tropical savanna. *EcoEvoRxiv* <https://doi.org/10.32942/X2WG75>
706 Zanne, A.E., Flores-Moreno, H., Powell, J.R., Cornwell, W.K., Dalling, J.W., Austin, A.T., Classen,
707 A.T., Eggleton, P., Okada, K., Parr, C.L., Adair, E.C., Adu-Bredu, S., Alam, A., Alvarez-
708 Garzón, C., Apgaua, D., Aragón, R., Ardon, M., Arndt, S.K., Ashton, L.A., ... Curran, T.J.
709 (2022). Termite sensitivity to temperature affects global wood decay rates. *Science*, 377, 1440–
710 1444. <https://doi.org/10.1126/science.abo3856>
711 Zeps, M., Senhofa, S., Zadina, M., Neimane, U., & Jansons, A. (2017). Stem damages caused by
712 heart rot and large poplar borer on hybrid and European aspen. *Forestry Studies*, 66, 21–26.
713 <https://doi.org/10.1515/fsmu-2017-0003>
714 Zhou, L., Dai, L., Gu, H., & Zhong, L. (2007). Review on the decomposition and influence factors of
715 coarse woody debris in forest ecosystem. *J. For. Res.*, 18(1), 48–54.
716 <https://doi.org/10.1007/s11676-007-0009-9>
717
718
719
720
721
722
723
724
725
726
727
728
729
730
731
732
733

734 **Supplementary Materials**735 Supplementary Table 1. Species composition and site descriptions for Pennyweight (PNW) and Station
736 Creek (STCK) biomass plots.

Site	Annual Rainfall (mm)	Species	Family	Stem Abundance (%)	Biomass (Mg)	Biomass (%)
PNW	812	<i>Eucalyptus cullenii</i>	Myrtaceae	86	2.24	96.4
		<i>Melaleuca stenostachya</i>	Myrtaceae	8	0.05	2.3
		<i>Terminalia aridicola</i> subsp. <i>chillagoensis</i>	Combretaceae	4	0.02	0.7
		<i>Gardenia vilhelmii</i>	Rubiaceae	2	0.01	0.5
STCK	1728	<i>Eucalyptus cullenii</i>	Myrtaceae	30	10.0	65.3
		<i>Corymbia clarksoniana</i>	Myrtaceae	28	3.11	20.2
		<i>Acacia disparrima</i> subsp. <i>calidestris</i>	Fabaceae	12	0.40	2.6
		<i>Larsenaikia ochreatea</i>	Rubiaceae	12	0.14	0.9
		<i>Terminalia subacroptera</i>	Combretaceae	8	0.95	6.2
		<i>Santalum acuminatum</i>	Santalaceae	4	0.19	1.2
		<i>Ficus opposita</i>	Moraceae	2	0.03	0.2
		<i>Callitris intratropica</i>	Cupressaceae	2	0.10	0.6
		<i>Brachychiton diversifolius</i> subsp. <i>orientalis</i>	Sterculiaceae	2	0.42	2.7

737

738

739

740

741

742

743 Supplementary Table 2. Sample size of species measured for changes in internal damage at PNW and
 744 STCK sites.

Species	Site	Sampled stems	Wood density (g/cm ³)
<i>E. cullenii</i>	PNW	15	0.9770
<i>E. cullenii</i>	STCK	6	0.9770
<i>C. clarksoniana</i>	STCK	14	0.8453
<i>M. stenostachya</i>	PNW	10	0.7405

745
 746 Supplementary Table 3. Model summaries for the effect of vertical position and tree species on proportion
 747 and absolute amount damaged (corresponds with Figure 4a-d).

Response	Predictor	χ^2	df	p
Proportion damage	Drill height (cm)	2.80	1	0.09
	Species	13.44	2	0.001
Absolute amount damaged	Drill height (cm)	6.11	1	0.01
	Species	35.05	2	< 0.001

748
 749 Supplementary Table 4. Model summaries for the effect of vertical position and tree traits (DBH and
 750 wood density) on proportion and absolute amount damaged (corresponds with Figure 4e-f).

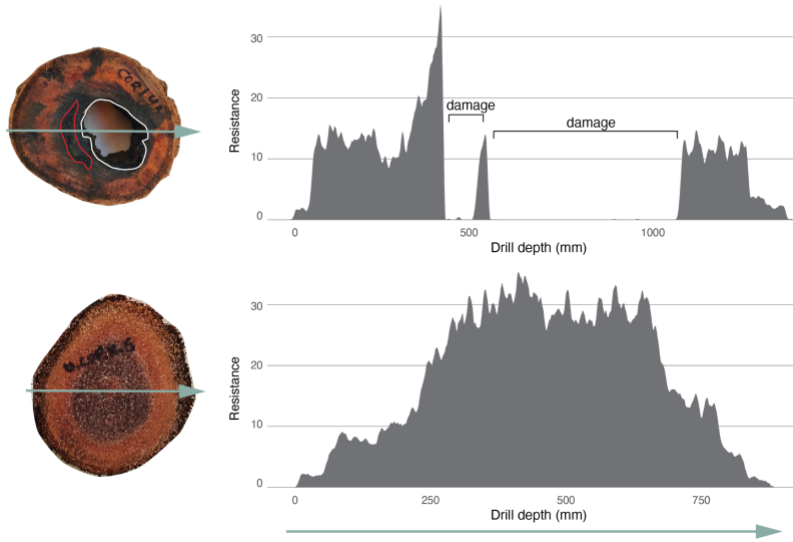
Response	Predictor	χ^2	df	p
Proportion damage	Drill height (cm)	2.61	1	0.11
	DBH (cm)	0.09	1	0.76
	Wood density (g cm ⁻³)	0.63	1	0.43
Absolute amount damaged	Drill height (cm)	5.48	1	0.02
	DBH (cm)	96.45	1	< 0.001
	Wood density (g cm ⁻³)	0.15	1	0.70

751

752 Supplementary Table 5. ANOVA table for species-level differences in DBH.

Response	df	SS	MS	F-value	p
Species	2	533	226.5	7.7	0.001
Residuals	41	1425	34.76		

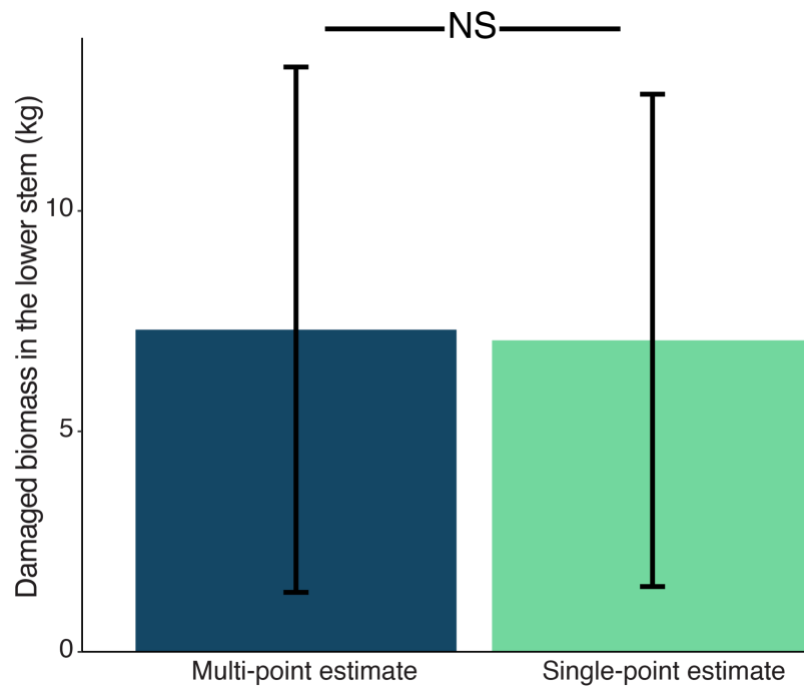
753



754

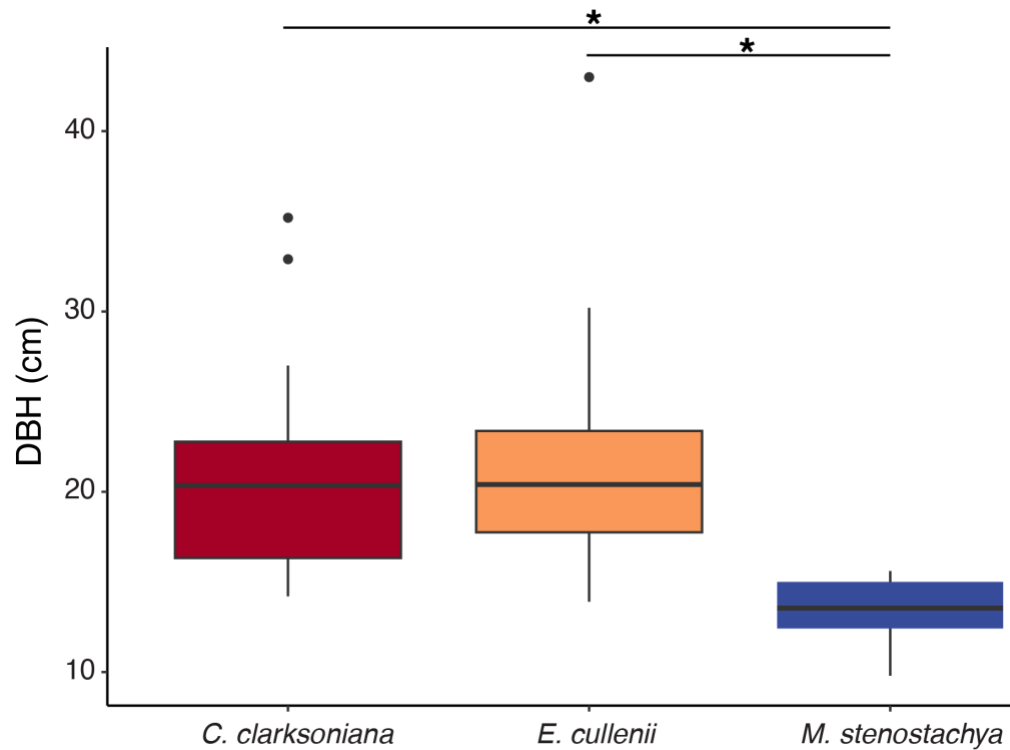
755 Supplementary Figure 1. Residril trace paired with a cross section photo of the stem segment that the
756 trace was taken from (Yatsko et al., 2024). Drill depth is represented on the X axis, with the measurement
757 beginning at X = 0 and ending at the diameter of the tree. The Y axis represents resistance, where high
758 values indicate sound wood and low values indicate damaged wood. The top trace shows a damaged cross
759 section (microbial damage is outlined in red and termite damage is outlined in white); on the residril
760 trace, decreases in resistance indicate segments with internal damage. The bottom trace depicts a sound
761 cross section, where resistance does not drop off as the drill passes through the tree stem.

762



763
764
765
766

Supplementary Figure 2. Comparison of damaged biomass in the lower stem estimated from a multi-sample method (blue) and a single-sample method (green). Error bars indicate \pm standard deviation.



767
768

Supplementary Figure 3. Species-level differences in diameter at breast height (DBH).